https://doi.org/10.5194/bg-2020-7
Preprint. Discussion started: 10 February 2020

Biogeosciences Discussions

Evaluating two soil carbon models within a global land surface model using surface and spaceborne observations of atmospheric CO_2 mole fractions

Tea Thum[1], Julia E. S. M. Nabel[2], Aki Tsuruta[3], Tuula Aalto[3], Edward J. Dlugokencky[4], Jari Liski[3], Ingrid T. Luijkx[5], Tiina Markkanen[3], Julia Pongratz[6], Yukio Yoshida[7], and Sönke Zaehle[1]

[1]Max Planck Institute for Biogeochemistry, Jena, Germany
[2]Max Planck Institute for Meteorology, Hamburg, Germany
[3]The Finnish Meteorological Institute, Helsinki, Finland
[4]NOAA ESRL Global Monitoring Division, Boulder CO, United States
[5]Meteorology and Air Quality Group, Wageningen University and Research, Wageningen, The Netherlands
[6]Department of Geography, Ludwig-Maximilians-Universität, Munich, Germany
[7]Center for Global Environmental Research, National Institute for Environmental Studies, Tsukuba, Japan

Correspondence: Tea Thum (tthum@bgc-jena.mpg.de)

Abstract. The trajectories of soil carbon (C) in the changing climate are of utmost importance, as soil carbon is a substantial carbon storage with a large potential to impact the atmospheric carbon dioxide (CO_2) burden. Atmospheric CO_2 observations integrate all processes affecting C exchange between the surface and the atmosphere. Therefore they provide a benchmark for carbon cycle models. We evaluated two distinct soil carbon models (CBALANCE and YASSO) that were implemented to a global land surface model (JSBACH) against atmospheric CO_2 observations. We transported the biospheric carbon fluxes obtained by JSBACH using the atmospheric transport model TM5 to obtain atmospheric CO_2. We then compared these results with surface observations from Global Atmosphere Watch (GAW) stations as well as with column XCO_2 retrievals from the GOSAT satellite. The seasonal cycles of atmospheric CO_2 estimated by the two different soil models differed. The estimates from the CBALANCE soil model were more in line with the surface observations at low latitudes (0° N-45° N) with only 1 % bias in the seasonal cycle amplitude (SCA), whereas YASSO was underestimating the SCA in this region by 32 %. YASSO gave more realistic seasonal cycle amplitudes of CO_2 at northern boreal sites (north of 45° N) with underestimation of 15 % compared to 30 % overestimation by CBALANCE. Generally, the estimates from CBALANCE were more successful in capturing the seasonal patterns and seasonal cycle amplitudes of atmospheric CO_2 even though it overestimated soil carbon stocks by 225 % (compared to underestimation of 36 % by YASSO) and its predictions of the global distribution of soil carbon stocks was unrealistic. The reasons for these differences in the results are related to the different environmental drivers and their functional dependencies of these two soil carbon models. In the tropical region the YASSO model showed earlier increase in season of the heterotophic respiration since it is driven by precipitation instead of soil moisture as CBALANCE. In the temperate and boreal region the role of temperature is more dominant. There the heterotophic respiration from the YASSO model had larger annual variability, driven by air temperature, compared to the CBALANCE which is driven by soil

https://doi.org/10.5194/bg-2020-7
Preprint. Discussion started: 10 February 2020


Biogeosciences Discussions Open Access EGU

temperature. The results underline the importance of using sub-yearly data in the development of soil carbon models when they are used in shorter than annual time scales.

1 Introduction

The global carbon (C) balance is mainly influenced by terrestrial and oceanic carbon fluxes. Since the early 1960s, when accurate measurements of atmospheric CO_2 began, the land and ocean have absorbed approximately half of annual anthropogenic carbon dioxide (CO_2) emissions (Le Quéré et al., 2018). The terrestrial natural carbon cycle consists of uptake by vegetation and release of carbon by plants' autotrophic respiration, soil decomposition by heterotrophic organisms and natural disturbances (Bond-Lamberty et al., 2016). At global scale, recent advances in remote sensing have allowed global spatially distributed estimates for gross primary production (GPP) generated together with machine learning methods (Tramontana et al., 2016). Photosynthesis takes place in the green plant parts, which can be detected from space as well as the sun-induced chlorophyll fluorescence that is related to photosynthesis (MacBean et al., 2018). Release of carbon from the terrestrial biosphere remains more elusive, since below ground processes cannot be directly detected globally and the understanding of the below ground processes is still developing (Bradford et al., 2016).

For soil respiration, including both autotrophic respiration by roots and heterotrophic respiration, some global datasets have been developed (Bond-Lamberty and Thomson, 2010; Hashimoto et al., 2015). Recently efforts to estimate heterotrophic respiration have also been made using machine learning techniques, Tang et al. (2019) and Warner et al. (2019) being the first attempts. The separation of heterotrophic respiration from the autotrophic respiration remains still a challenge and in these two studies it has been done at yearly scales. The soil stores twice as much carbon as the atmosphere (Scharlemann et al., 2014) and its fate in changing climate remains uncertain (Crowther et al., 2016). To have reliable predictions of future carbon stocks, process-based understanding of the below ground carbon cycle needs to be achieved.

Heterotrophic respiration, R_h, at global scale is a very important part of the carbon cycle. It is influenced by moisture and temperature conditions (Wei, 2010). In many global modelling approaches, moisture and temperature dependencies are influencing a first-order decay process of soil carbon pools (Todd-Brown et al., 2013). The magnitude of modelled R_h is therefore dependent on these parameters, the pool sizes and their turnover rates as well as the incoming litter input from vegetation. The role of the turnover rate is crucial, as the pre-industrial turnover rates are the key uncertainty in simulation of soil organic matter stocks for the 21st century (Todd-Brown et al., 2014). Soil carbon modelling needs improvements so that future changes in soil carbon stocks can be better predicted (Bradford et al., 2016). Current global carbon cycle models give a wide range of estimates for changes in soil carbon by the end of this century (Todd-Brown et al., 2014). There is currently ongoing development of soil carbon models, and these next generation models include detailed microbial dynamics with nutrient cycles (Wieder et al., 2018; Yu et al., 2019).

https://doi.org/10.5194/bg-2020-7
Preprint. Discussion started: 10 February 2020


Biogeosciences Discussions Open Access EGU

One way to benchmark soil carbon models has been by using observations of soil carbon stocks (Todd-Brown et al., 2013). At smaller scales, gas exchange observations with chambers have also been used (Ťupek et al., 2019). It is anyhow challenging to find reasons for differences in heterotrophic respiration between large scale models, as the litter input to the soil influences heterotophic respiration and this litter input varies between the models. Alternative way forward is to use a test-bed for these models, as done by Wieder et al. (2018).

An alternative, regionally integrated approach is using observations of the atmospheric CO_2, which integrate all processes involved in global surface-atmosphere C exchange. The surface observation network of atmospheric CO_2 has been used in benchmarking global carbon cycle models (Cadule et al., 2010; Dalmonech and Zaehle, 2013; Peng et al., 2015). Recent advances of satellite technology have enabled retrievals of space-born dry-air total column-averaged CO_2 mole fraction (XCO_2), quantifying CO_2 in the entire atmospheric column between the land surface and the top of the atmosphere. These observations reveal a more spatially integrated CO_2 signal compared to surface site observations and together they provide a complementary dataset. These two data sources have been used together to study the carbon cycle with "top-down“ inversion modelling (Crowell et al., 2019). This kind of modelling framework uses atmospheric CO_2 observations to constrain a priori biospheric and ocean fluxes, based on the Bayesian inversion technique, which results in optimized estimates (a posteriori) of the fluxes (Maksyutov et al., 2013; Rödenbeck et al., 2003; van der Laan-Luijkx et al., 2017; Wang et al., 2019). The estimates for fossil emissions are often assumed as known, i.e., not optimized in the inversion.

In this study we investigate in how far atmospheric CO_2 observations, both from surface network and space-born observations, can be used to benchmark these two soil carbon models included in the land surface model JSBACH, one of the models participating in CMIP6. Previous studies evaluating the new YASSO soil carbon model performance when implemented in JSBACH, have shown better performance in relation to observations of soil carbon stocks when compared to the older soil carbon model of JSBACH, CBALANCE (Goll et al., 2015; Thum et al., 2011). Since the only difference between the two model versions is the description of the underlying soil processes and include no major feedbacks between soil and vegetation in the model set-up (excluding the effect of litter accumulation on fire fluxes), the difference in the release of carbon to the atmosphere originates only from the soil carbon models. The two soil carbon models used in this work have different environmental drivers. CBALANCE has soil moisture and soil temperature as driving variables and the YASSO model precipitation and air temperature. The models have differing response functions to these environmental variables as well as different carbon pool structures, and they are both first-order decay models. This framework allows us to investigate how these above-mentioned differences in soil carbon modes influence atmospheric CO_2. To transfer terrestrial carbon fluxes from the surface to the atmosphere, we use the transport model TM5 and the anthropogenic and ocean fluxes from an inversion framework (van der Laan-Luijkx et al., 2017). In the analysis we also use a simple box model calculation to further understand the main causes in the different outcomes of the models.

https://doi.org/10.5194/bg-2020-7
Preprint. Discussion started: 10 February 2020


Biogeosciences Discussions Open Access EGU

2 Materials and Methods

We used the land surface model JSBACH (Mauritsen et al., 2019) to obtain the net land-atmosphere CO_2 exchange and fed them together with ocean, fossil and land use fluxes into a transport model TM5, which simulates the resulting atmospheric CO_2 mole fractions at selected surface stations as well as column integrated values for comparison to satellite derived column CO_2.

2.1 Model simulations: JSBACH with two soil carbon models

JSBACH is the global land surface model of the Max Planck Institute's Earth System Model (Mauritsen et al., 2019), simulating the terrestrial carbon, energy and water cycles (Reick et al., 2013). In this study JSBACH was run with two different sub-models for soil carbon that are described below. The older model, CBALANCE, has been used in CMIP5 simulations of JSBACH (Giorgetta et al., 2013) and the newer model, YASSO, has been used in simulations for the annual global carbon budget (Le Quéré et al., 2015; Le Quéré et al., 2018) and is used in CMIP6 simulations of JSBACH (Mauritsen et al.,2019). It is furthermore also used in JSBACH4, a re-implementation of JSBACH for the ICON-ESM (Giorgetta et al., 2018; Nabel et al., 2019).

Independent of the used sub-model for soil carbon, JSBACH uses three carbon pools for the living vegetation carbon: a wood pool, containing woody parts of plants, and a green and a reserve pool containing the non-woody parts. JSBACH simulates different processes that lead to losses from the vegetation pools, such as grazing, shedding of leaves and natural or anthropogenic disturbances. Depending on the process, some of the vegetation carbon is lost as CO_2 into the atmosphere, while the remaining part is transferred as dead vegetation into the litter and soil pools of the used sub-model for soil carbon, where it is then subject to the internal processes of the soil carbon sub-model. The only process outside of the soil carbon sub-model which influences dead material are the fire processes, burning parts of above ground litter carbon.

2.1.1 The soil carbon model CBALANCE

CBALANCE (CBA) is the original soil carbon sub-model of JSBACH (Raddatz et al., 2007), which has been used in CMIP5. The environmental drivers for decomposition in CBA are soil temperature (at soil depth of 30 to 120 cm below the surface) and a relative soil moisture (α) of the upper-most soil layer, which is 5 cm thick. The α varies between zero and one.

The function for soil temperature dependence, $f_{CBA,T_{soil}}$ of decomposition follows a Q10 formulation as

$$f_{CBA,T_{soil}}(T_{soil}) = Q_{10}^{\frac{T_{soil}}{10^oC}} \quad (1)$$

with a Q_{10} value of 1.8 and T_{soil} is soil temperature in Celsius (shown in Fig. S1a) (Raddatz et al., 2007). The dependency on relative soil moisture α is linear (Fig. S1 b) and it is calculated as

$$f_{CBA,\alpha}(\alpha) = MAX(\alpha_{min}, \frac{\alpha - \alpha_{crit}}{1.0 - \alpha_{crit}}) \quad (2)$$

where α_{crit} is 0.35 and α_{min} is 0.1 (Knorr, 2000).

https://doi.org/10.5194/bg-2020-7
Preprint. Discussion started: 10 February 2020


Biogeosciences Discussions Open Access EGU

Together these functions are modulating the rate of decomposition, so that the R_h from each pool (denoted by i) is

$$R_h(T_{soil}, \alpha) = f_{CBA,\alpha} f_{CBA,T_{soil}} \frac{C_i}{\tau_i} \quad (3)$$

where C_i is the carbon content of each pool and τ_i is the turnover rate of each pool in days. CBA uses five different carbon pools having different turnover times:

- Two green litter pools: one above- and one below ground in which the non-woody plant parts are decomposed with turnover times between 1.8 and 2.5 years (Goll et al., 2015)
- Two woody litter pools: one above- and one below ground in which the woody plant parts are decomposed with turnover times of several decades
- One slow pool receiving its input from the four litter pools and its turnover time is in the order of a century.

2.1.2 The soil carbon model YASSO

The original soil carbon model of JSBACH was replaced by YASSO (YAS) (Thum et al., 2011; Goll et al., 2012). JSBACH's YAS implementation is based on the Yasso07 model (Tuomi et al., 2009). Development of Yasso07 has relied heavily on litter bag and other observational data sets that have been used to estimate the model parameters (Tuomi et al., 2009, 2011). Owing to its strong connection to experiments, its environmental drivers are quasi-monthly air temperature and precipitation.

The decomposition dependency on air temperature is

$$f_{YAS,T_{air}}(T_{air}) = e^{\beta_1 T_{air} + \beta_2 T_{air}^2} \quad (4)$$

where T_{air} is air temperature (°C), parameter β_1 is 9.5 $\times$ 10^{-2} $^\circ C^{-1}$ parameter β_2 is -14 $\times$ 10^{-4} $^\circ C^{-2}$ (Fig. S1c).

The decomposition depends on precipitation P_a (m) as

$$f_{YAS,P_a}(P_a) = (1 - e^{\gamma P_a}). \quad (5)$$

where γ = -1.21 m^{-1} (Fig. S1d). The environmental drivers for YAS (precipitation and air temperature) are averaged for a 30-day period.

Similar to CBA, YAS has slowly and fast decomposing pools, but its pool dynamics are more structured. YAS uses 18 carbon pools, nine for the decomposition of woody litter and nine for the decomposition of non-woody litter. The only difference in the calculation of the decomposition rates between non-woody and woody pools is an additional parameter that increases the turnover rates with increasing size of the woody litter (Tuomi et al., 2011). In addition to the distinction into woody and non-woody litter which is also done in CBA, YAS takes the chemical composition of the litter into account. YAS uses four chemically distinct pool kinds: acid soluble, water soluble, ethanol soluble and non-soluble. For each of these four chemical compositions one above and one below ground pool are used. In addition there is one humus pool for woody and one for non-woody material. The dynamics of the YAS carbon pools are described in (Tuomi et al., 2009) with decomposition fluxes

https://doi.org/10.5194/bg-2020-7
Preprint. Discussion started: 10 February 2020


Biogeosciences Discussions Open Access EGU

causing redistributions among the different pools or losses to the atmosphere. Each of the pools has a decay constant, which is modified by the environmental dependencies in Eqs. (4) and (5).

Each PFT used in JSBACH has a distinct chemical composition. Furthermore, the branch size of the woody litter is PFT-dependent.

2.2 The model simulations: The JSBACH set-up

JSBACH model simulations followed the TRENDY v4 protocol in terms of JSBACH version, simulation protocol and forcing data (Le Quéré et al., 2015; Sitch et al., 2015). Climate forcing was based on CRUNCEP v6 (Viovy, 2010) and the global atmospheric CO_2 was obtained from ice core and NOAA monitoring station data (Sitch et al., 2015). For both set-ups the model was separately run into equilibrium, i.e. until the soil carbon pools of the applied carbon sub-model were at steady-state. The two different transient simulations were then done for the period 1860 to 2014. Anthropogenic land cover change was forced by the LUHv1 dataset (Hurtt et al., 2011) and was simulated as described in Reick et al. (2013). While fire and windthrow were simulated, natural land cover changes and the nitrogen cycle were not activated. Simulations were done at T63 spatial resolution (approximately 1.9°, 200 km). For further details on the spin-up and the model version please refer to the SI.

2.3 The model simulations: TM5

To estimate atmospheric CO_2, we used the global Eulerian atmospheric transport model TM5 (Krol et al., 2005; Huijnen et al., 2010). TM5 was run globally at 6° x 4° (latitude x longitude) resolution with two-way zoom over Europe, where the European domain was run at 1° x 1° resolution. This is the pre-existing set-up that was readily available. The 3-hourly meteorological fields from ECMWF ERA-Interim (Dee et al., 2011) were used as constraints. Linear interpolation was done to obtain CO_2 estimates at the exact locations and times of the observations.

We fed TM5 with daily biospheric, weekly ocean and annual fossil fuel fluxes to obtain realistic atmospheric CO_2. Values of GPP and total ecosystem respiration were taken from the JSBACH simulations for the two different soil model formulations. Also, carbon release from vegetation and soil owing to land-use change, fires and herbivores were taken from the JSBACH model results as part of terrestrial biosphere carbon fluxes. In addition, we used the posterior biospheric flux estimates from CarbonTracker Europe (CTE2016, later referenced to as CTE; van der Laan-Luijkx et al. (2017)) to provide some guidance on the ability of TM5 to represent the individual site observations. The ocean fluxes were the a posterior estimates from the same study.

Fossil fuel emissions are from the EDGAR4.2 Database (EDGAR4.2, 2011) and Carbones project (http://www.carbones.eu), with scaling to global total values as for the Global Carbon Budget as described in van der Laan-Luijkx et al. (2017). The annual fossil fuel flux to the atmosphere was approximately 8.63 $PgCyr^{-1}$, and ocean uptake of carbon was approximately 2.33 $PgCyr^{-1}$ when averaged over years 2001-2014. Annual values are summarized in Table S1.

Simulations with TM5 were done for 2000-2014, but the first year was considered as spin-up and omitted from the analysis.

https://doi.org/10.5194/bg-2020-7
Preprint. Discussion started: 10 February 2020


Biogeosciences Discussions Open Access EGU

2.4 The surface observations

Surface observations of atmospheric CO_2 from NOAA weekly discrete air samples (ObsPack product: GLOBALVIEWplus v2.1; ObsPack (2016)) were used to evaluate the effect of different soil carbon models on tropospheric atmospheric CO_2 seasonal cycles at sites around the globe. The sites used in the evaluation are shown in Fig. 1. From the data, samples reflective of well-mixed background air were selected (based on flag criteria) similar to van der Laan-Luijkx et al. (2017) to minimize the influence on the observation of transport model errors in our analysis.

2.5 The satellite retrievals

GOSAT (Greenhouse Gases Observing Satellite) from Japan Aerospace Exploration Agency (JAXA) was launched in 2009 and observes column XCO_2 with the TANSO-FTS instrument (Kuze et al., 2009). These data were used to evaluate the different simulations and to assess the model performance at larger spatial scale.

XCO_2 from the simulation results were calculated using global 4° x 6° x 25 (latitude x longitude x vertical levels) daily average 3-dimensional (3-D) atmospheric CO_2 fields. For each satellite retrieval, the global 3-D daily mean gridded atmospheric CO_2 estimates were horizontally interpolated to the location of the retrievals to create the vertical profile of simulated CO_2. Averaging kernels (AKs) (Rodgers and Connor, 2003) were applied to model estimates to ensure reliable comparison with GOSAT retrievals:

$$\hat{C} = c_a + (\boldsymbol{h} \circ \boldsymbol{a})^T (\boldsymbol{x} - \boldsymbol{x}_a), \tag{6}$$

where $\hat{C}$ is XCO_2, scalar c_a is the prior XCO_2 of each retrieval, $\boldsymbol{h}$ is a vertical summation vector, $\boldsymbol{a}$ is an absorber-weighted AK of each retrieval, $\boldsymbol{x}$ is a model profile and $\boldsymbol{x}_a$ is the prior profile of the retrieval. Each retrieval had a prior profile (Yoshida et al., 2013). The retrievals for different terrestrial TransCom (TC) areas (Fig. 1) were compared with those calculated from the two model simulations. For comparison with GOSAT XCO_2, the estimates of 3D fields at 6° x 4° resolution were used, but not those from the zoom grids due to technical reasons. Differences in XCO_2 due to model resolution were not significant within the context of this study. In this work GOSAT observations (NIES retrieval V02.21 and V02.31) between July 2009 and the end of 2014 were used.

3 Results

3.1 Global carbon stocks and fluxes with the two model formulations

Since the two different model formulations differ only in their soil carbon module formulation, the incoming flux to the ecosystem from photosynthesis is the same in both cases. Analysis of the results was done for 2001-2014, and we show here averaged values for that period.

Global simulated GPP of 167 PgCyr^{-1} (Table 2) is highly overestimated when compared to the upscaled data product from FLUXCOM, which is giving a mean value of 126 PgCyr^{-1} for this time period (Jung et al., 2019) and having a range

https://doi.org/10.5194/bg-2020-7
Preprint. Discussion started: 10 February 2020


Biogeosciences Discussions Open Access EGU

of 106-130 PgCyr^{-1} for a longer time period. Despite the overestimate of global GPP by the model, the comparison to the FLUXCOM product shows that the seasonal cycles in different latitudinal regions are quite similar, although in the northern boreal region JSBACH reaches maximum GPP values later than the FLUXCOM product (Fig. S4). Vegetation carbon biomass was similar in both model formulations (Table 1). The small difference is caused by fire fluxes, which have small differences in their magnitude but similar spatial patterns (Fig. S3). The global estimate for total soil carbon by CBA was 4.5-fold larger than by YAS (Table 1). The global estimate for the litter simulated by YAS pool was larger than that simulated by CBA.

The net CO_2 flux shows a slightly larger land sink for YAS than CBA (Table 2). Owing to the larger litter pool, fire fluxes are larger in the YAS model formulation by 0.50 PgCyr^{-1}. This caused the heterotrophic respiration of YAS to be 0.56 PgCyr^{-1} smaller than by CBA, since the model was spun-up to steady state in 1860. This does not completely compensate for the difference and leads to a small discrepancy in net CO_2 fluxes between the two model formulations.

Since the soil carbon pools are of very different magnitude, but the annual R_h between the model formulations are similar, the turnover times of the two formulations must differ. The turnover times (τ) of soil carbon pools can be evaluated at both grid scale and from global values. This global value is obtained by dividing the total soil carbon pool (to which both soil and litter carbon stocks are added) by the annual R_h. Calculated from the global values averaged between 2001 and 2014, the apparent turnover time for CBA is 51.3 years and for YAS 14.8 years. The anomalies of the turnover times are represented in Fig. S4. These have been calculated from the carbon pools over the whole time period and the mean annual R_h. The models show longer turnover times in northern high latitudes and dry areas. CBA predicts longer turnover times to southern Europe, whereas YAS does not. On the other hand, YAS predicts longer turnover times close to Saharan desert, different to CBA. YAS also consistently predicts longer turnover times to northern latitudes, but CBA does not do this for the northern European region.

The global distribution of soil carbon is very different between the model formulations (Fig. 2). Overall the CBA values are higher, with the highest values reaching over 105 kgCm^{-2}, being four times larger than the values predicted by YAS. The CBA model has large values of soil carbon in the mid-latitudes of the Northern Hemisphere. YAS predicts larger values in the temperate region of the Northern Hemisphere, but the highest values of soil carbon are located in arctic regions.

Even though annual total global values of heterotrophic respiration are similar between the different model formulations, their global seasonal cycles are different (Fig. 3). The YAS version has a 66 % larger variation of R_h during the year than CBA. Both model versions have their minimum value of R_h in February. While CBA has a maximum in August, YAS reaches its maximum value one month earlier, and global R_h also stays high during August. YAS clearly has a steeper increase and decline in its seasonal cycle than CBA. The R_h seasonal cycles show clear differences in their seasonal pattern between the two model formulations in different latitudinal regions (Fig. 4). The magnitude of heterotrophic respiration is quite similar in the different latitudinal zones. The YAS model shows however a larger amplitude in the seasonal variation in all of the regions.

The seasonal cycle is quite different between the model formulations in the tropics. At 0° N-30° N, where YAS has seasonal cycle shifted earlier compared to CBA. In this region YAS has 42 % larger seasonal amplitude of R_h than CBA. In the two more northern regions in the Northern Hemisphere the amplitude in R_h of YAS is approximately twice the amplitude of CBA. In both of these regions YAS has clear maximum values of R_h in July and August, while the seasonal cycles of CBA are more shallow and do not include such clear maximums.

https://doi.org/10.5194/bg-2020-7
Preprint. Discussion started: 10 February 2020


Biogeosciences Discussions Open Access EGU

In the southern hemisphere in regions 0° S -10° S and 10° S -30° S the CBA predicts higher values of R_h during the first months of the year after which it stays lower until the end of the year, whereas YAS shows a clear lowering between June and September. In the region 10° S -30 ° S YAS has 54 % larger amplitude in R_h than CBA.

The variation in R_h seasonal dynamics of these two model formulations can be linked to the differences in their environmental drivers and functions. In Table 3 the correlation between heterotrophic respiration and the environmental drivers of each specific model formulation are shown for the different latitudinal regions. Figures S5-S8 show these same relationships. The R_h from CBA has a strong correlation with the soil moisture α in the tropical region (30° S-30° N) and a high correlation with the soil temperature T_{soil} in the northern high latitudes (30° N-90° N) and lower correlation in southern high latitudes (30° S-60° S). In other regions the r^2 values are low between R_h from CBA and its environmental drivers and in two regions the dependency between α and R_h is negative. On the other hand, the R_h predicted by the YAS model shows strong correlation to its environmental drivers (Table 3). The r^2 values between R_h and precipitation are over 0.80 in all regions except region 30° S-60° S. Between the air temperature and R_h the results are similar, with the only lower r^2 value taking place in tropics in the Southern Hemisphere. The seasonal cycle of R_h predicted by the YAS model does not show any positive correlation to soil moisture variable α in any of these regions (Table 3 and Fig. S9). In the tropical region the soil moisture for CBA and precipitation for YAS are more important drivers compared to soil and air temperatures. In the high latitudes the temperature has larger effect on R_h with both models, even though in the Northern Hemisphere also the precipitation has a significant role for YAS.

To assess, whether the higher amplitude of the seasonal cycle in R_h by YAS is caused by the larger litter pool or the environmental response functions, a simple box model calculation was performed (a detailed description in Appendix).

When the global respiration was calculated with the turnover times and soil carbon pools of the YAS model, but using the environmental responses and drivers of the CBA model, the annual magnitude decreased by 29 % compared to the original YAS model (Table A1). However, the yearly maximum value did not change by much. When the opposite was done, and the turnover time and soil carbon pools of CBA were used with the environmental responses and inputs of the YAS model, the magnitude of the global heterotrophic respiration was increased approximately 1.4-fold (Fig. A1). The increase in the amplitude was 83 % (Table A1). Therefore this simple analysis suggests that the environmental variables and their response functions cause the larger global amplitude of R_h in the YAS model formulation. To further disentangle, whether this change was caused by the different environmental drivers or their functional dependencies, we made additional tests.

The amplitudes of the seasonal cycle of R_h (difference between the maximum and minimum values) are shown in Table A1. For the YAS model, there happens a strong decrease in the amplitude when both driver variables and the response functions are changed. When only driver variables are changed, there occurs only a slight decrease. When the response functions are changed, the decrease in the amplitude is more pronounced with 21 %. The amplitude predicted by the CBA model increases, when the driving variables and response functions are changed (Table A1). This increase is occurs when either driving variables or response functions are changed individually. However, with the change of the response functions the change in the amplitude is larger, 74 %. Therefore the response functions have a more pronounced role in the changes than only the driving variables and this was true for both of the models.

https://doi.org/10.5194/bg-2020-7
Preprint. Discussion started: 10 February 2020

3.2 Evaluation against surface observations

Seasonal cycle amplitudes (SCAs) of atmospheric CO_2 are successfully simulated by the modeling framework across different latitudes (Fig. 5a). The r^2 values of the observed seasonal cycle and the model estimates are high across latitudes, despite some lower values in mid-latitudes of the Northern Hemisphere (Fig. 5b). Averaged over all the latitudes the r^2 value, calculated as linear correlation of simulated and observed averaged annual cycles, was 0.93 for the CTE, 0.90 for CBA and 0.87 for YAS.

The CBA model is able to capture the timing of the seasonal cycle in northern latitudes, but has a tendency to overestimate the SCA by 30 % north of 45° N. In this region the underestimation of SCA by CTE is approximately 5 % and by YAS 14 %. In the region 0° N-45° N the YAS underestimates the SCA in average approximately by 32 %, whereas CTE underestimates it by 4 % and CBA overestimates it only by 1 %. The agreement between estimated atmospheric CO_2 and observations was worse in YAS than in CBA when considering the r^2 value and the seasonal cycle. Overall, the magnitude of the SCA predicted by YAS had less bias north from 45° N compared to CBA, but large underestimation in latitudes 0° N-45° N, where CBA was very successful in attaining the right SCA.

This behavior is further illustrated from comparisons of the detrended seasonal cycle at four stations in the Northern Hemisphere (Fig. 6 and Table S2). To confirm the general quality of the TM5 model used for both YAS and CBA we plotted its biospheric posterior fluxes from CarbonTracker Europe 2016 (CTE); indeed, deviations of CTE to observations are much smaller than from the JSBACH model at all sites. At the high-latitude sites, Alert and Pallas (Fig. 6a, b), CBA overestimates the seasonal cycle amplitude, while YAS shows some phase-shift of the cycle. The observed SCAs are smaller at the two more southern sites, Niwot Ridge and Mauna Loa. For those sites, CBA is generally successful in capturing their magnitude (Table S2), whereas YAS underestimates them strongly. YAS is also having difficulty capturing the seasonal pattern at Niwot Ridge. This was happening generally in the temperate region, as is also seen in the lower r^2 values of the YAS model at the different sites (Fig. 5.

When comparing the overall bias at these four sites between the observations and the model simulations, CBA overestimated CO_2 by 3.65 ppm and YAS by 2.27 ppm, when averaged over all the measurements within the study period. A closer look at the bias at Mauna Loa (Fig. S10) revealed a trend in this bias between year 2000 and 2014. The CTE shows no bias. The CBA is overestimating CO_2 by 1.76 ppm in the beginning and by 3.74 ppm in 2014. The YAS has lower overestimation, being 1.12 ppm in 2000 and 3.14 in 2014.

The results at surface sites show that CBA largely overestimated SCA at high northern latitudes, whereas YAS almost consistently underestimated the SCA in the Northern Hemisphere. CBA captured the seasonal cycle patterns better than YAS across different latitudes.

3.3 Column XCO_2 comparisons for TransCom regions

This evaluation of the two soil modules against satellite column XCO_2 was carried out for the different TransCom (TC) regions (Fig. 1). The comparison was based on seasonal cycle amplitudes and r^2 values similar to the surface site evaluation. Not all the TC regions show a clear seasonal cycle, such as regions in South America (TC regions 3 and 4), northern part of Africa (TC=5)

https://doi.org/10.5194/bg-2020-7
Preprint. Discussion started: 10 February 2020

and Australia (TC=10). For completeness we show the analysis also for these regions in Table S3. For regions with clear seasonal cycle we used the ccgcrv curve fitting procedure available from NOAA (https://www.esrl.noaa.gov/gmd/ccgg/mbl/crvfit/crvfit.html, (Thoning et al., 1989)), but for regions with missing data or no clear seasonal cycle, we averaged over all years of data.

To further illustrate the results from this comparison, we show data for two regions having a clear seasonal cycle and reflecting the same behaviour that was noticed at the four surface observation sites that were looked deeper into in the previous section. In TC region 2, the southern part of North America, CBA is more successful in capturing the observed SCA than YAS (Fig. 7 a), even though CBA reaches the minimum XCO_2 later than observations. YAS underestimates SCA by 56% and has a different seasonal pattern than observations, so the minimum is reached earlier than in the observations and also the shape during the summer period is different to the observations. In TC region 11, Europe, both models capture the SCA (Fig. 7, Table S3) and the seasonal cycle in the first part of the year. The increase of CO_2 is not as well captured by the simulations.

Overall, observed and simulated XCO_2 differ from each other similar to the surface site observations. Estimates of SCA by YAS are too small in mid-latitudes (Fig. 7a) and in TCs 2, 5 and 8 compared to the observations, and CBA is better in capturing the observed annual cycles. At TC=1 (the northern part of North America), CBA overestimates the SCA, while YAS better captures it. However, the seasonal cycle pattern is better captured with CBA (Table S2) than with YAS. Generally YAS had smaller SCAs than the observations and CBA was more consistent with the observations in most TC regions (Table S3). CBA is also better than YAS in capturing the seasonal pattern of XCO_2 in the all TC regions (Table S3).

There occurs bias between the space-born observations and the model simulations. When averaged over the time period used and the TC regions, CBA overestimates the GOSAT observations by 3.37 ppm and YAS by 2.33 ppm. These values were in line with the bias estimates at the four surface sites.

4 Discussion

In this work our aim was to use atmospheric observations to benchmark soil carbon models. Our main finding was that the two models predicted differently the annual cycle of the global R_h, with the YAS model having a larger amplitude. This in turn lead to pronounced clear differences in the model predictions of seasonal cycles of the atmospheric CO_2 mole fractions. To be able to attribute the differences between the two models we need to compare their results from different aspects and to also judge whether our model simulations are reasonable in the light of previous research.

Similarly to the earlier studies (Goll et al., 2015; Thum et al., 2011), in our results the YAS model was more successful than CBA in estimating the observed global soil carbon stocks, which is approximately 1500 PgC (Scharlemann et al., 2014) including large uncertainties. The distribution of soil carbon stocks was also more realistic in YAS than in CBA. The large soil carbon stocks in the mid-latitudes predicted by CBA (Fig. 2 a) are unrealistic compared to current estimates of global soil carbon distribution (Scharlemann et al., 2014). The large carbon stocks at high latitudes predicted by the YAS model (Fig. 2) are more in line with the observations. However, the version of JSBACH used does not include peatlands and is modelling only mineral soils, therefore the large carbon reservoirs of peatlands are not captured by the model, as they are now described

https://doi.org/10.5194/bg-2020-7
Preprint. Discussion started: 10 February 2020

as mineral soils. The YAS model is widely used in different applications at smaller scale and its performance to estimate soil carbon stocks has been found to be good (Hernández et al., 2017). Comparability between the model-calculated and the observed carbon stocks is relevant for any analyses of the carbon fluxes because in the both models the fluxes are proportional to the stocks (flux = decomposition rate * stock).

The global turnover rate of soil carbon by CBA was somewhat larger than in an earlier study, where it was estimated to be 40.8 years (Todd-Brown et al., 2014). This value was in the higher end of the CMIP5 models. The global turnover rate value from YAS, which was 14.8 years, is more in the range of the other CMIP5 models (Todd-Brown et al., 2014). The spatial distribution of the turnover rate anomalies show the the differences caused by the environmental drivers and their dependencies at annual timescales. When comparing these overall turnover rates of the total soil carbon, it is important to keep in mind that both models consisted of carbon pools that had widely varying turnover rates. For example, despite of the higher overall turnover rate, the turnover rate of the most recalcitrant carbon pool of YAS was an order of magnitude lower than that of CBA.

Moving to the monthly time scales, we can see that the global seasonal R_h cycle had a larger amplitude with YAS than with CBA (Fig. 3) and a simple box model calculation found the environmental drivers and their response functions to be the cause of this instead the large litter pool in the YAS model. It is anyhow challenging to further disentangle whether this larger amplitude is mainly caused by the differing environmental drivers the soil carbon models or if their functional dependencies would play a bigger role. The analysis by the box model suggested a stronger role of the response functions compared to the driving variables at monthly timescales, but strong conclusions cannot be drawn from such a simple analysis. Also other studies have showed that the response functions themselves lead to pronounced differences between soil carbon models (Wieder et al., 2018).

The annual heterotrophic respiration was 66.1 PgCyr^{-1} for CBA and 65.5 PgCyr^{-1} for YAS (Table 2), which falls in the range of estimates from the Earth System Models (41.3-71.6 PgCyr^{-1}) and is close the observation based estimates of 60 PgCyr^{-1} (Shao et al., 2013). The similar values of R_h by YAS and CBA are caused by the way the models are run into steady-state in the beginning of the simulation in 1860. Part of this difference is caused by the fire fluxes. The YAS model has a larger litter pool that behaves as fuel for fires. Therefore, to have the system at steady state, global heterotrophic respiration by YAS must be less. Also, the simulation time of 140 years before the beginning of the analysis might also cause some divergence between the model runs.

When R_h is compared by latitudinal zones, differences between the model formulations are visible in the variability and timing of the seasonal cycles in many regions (Fig. 4). R_h showed strong correlations to the environmental drivers of the models in different latitudinal zones (Table 3). Both models are largely influenced by their moisture dependency in the tropical region (Table 3). CBA is driven by soil moisture with a linear dependence and YAS is driven by precipitation. While at annual timescales these two variables (air vs. soil temperature and precipitation vs. soil moisture) are similar, since precipitation is affecting soil moisture and on longer timescales air temperature determines soil temperature in the top soil layers, the seasonal cycles of the variables are different. At annual timescales, at which the YAS model has been originally developed, the dynamics of these variables are not likely to be as different as at these shorter timescales. Precipitation begins earlier in the season in the tropical region, and it causes YAS to reach yearly maximum R_h earlier than CBA, which is driven by soil moisture in this

https://doi.org/10.5194/bg-2020-7
Preprint. Discussion started: 10 February 2020


Biogeosciences Discussions Open Access EGU

region. Also in the temperate region, where the temperature has a larger role, the air temperature has larger variability than soil temperature and this leads to different kind of seasonal pattern of the R_h predictions by the models.

Different moisture dependencies of R_h have earlier been found to be important (Exbrayat et al., 2013). At the global level Hursh et al. (2017) recommended using parabolic soil moisture functions in preference to functions based on mean annual precipitation. Their study considered soil respiration, i.e., autotrophic respiration by roots was also included. Ťupek et al. (2019) evaluated the YAS model against R_h observations at two coniferous sites in southern Finland and found problems in capturing the seasonality in the observations and the variability in the summertime fluxes. One reason for this they mention is the response of the simulated R_h to soil moisture conditions, since R_h is not attenuated in very moist conditions and they found a need to improve the moisture dependency of the YAS model. This is in line with our findings, that a model that has been parameterized at annual time scales requires further development before it can be reliably applied at shorter timescales. Precipitation has been originally used in the YAS model as a proxy for soil moisture, since enough accurate soil moisture observations for model development haven't been available. Clearly, this idea needs reconsideration as our results show that at zonal spatial scales and monthly temporal scale the R_h from YAS is not at all correlated to soil moisture variable α.

The global GPP, being 165 PgCyr^{-1} in this study, was overestimated, compared to the FLUXCOM estimate. Different FLUXCOM products give estimates between 106 and 130 PgCyr^{-1} for period 2008-2010 (Jung et al., 2019). There has been also other estimates for the global GPP. The Carbon Cycle Data Assimilation system provides a value of 146 ($\pm$ 19) (Koffi et al., 2012) and the estimates based on isotope observations have given estimates of 150 to 175 PgCyr^{-1} (Welp et al., 2011). The GPP of JSBACH is relatively high, but it was the same for both of the model formulations and only contributed to the amount of litter fall. Therefore we do not expect the variation of its magnitude to have substantial influence to our results, bearing also in mind that the seasonal cycle in different latitudinal zones was captured by the JSBACH model (Fig. S2).

The differences by the two models in the seasonal cycle of atmospheric CO_2 were strong. CBA better reproduced the seasonal cycle amplitudes capturing the shape of the seasonal cycle both for surface sites and comparisons in the TC regions, even though its soil carbon distribution had lower performance compared to YAS. CBA exaggerated the seasonal cycle amplitudes at high northern latitudes, as has been found earlier (Dalmonech and Zaehle, 2013).

The biases between XCO_2 from satellite retrievals and the model results originating from the JSBACH simulations are relatively large and this is likely caused by the use of a posteriori ocean fluxes from the CTE2016. The global a posteriori land sink (including biomass burning emissions) of CTE is approximately -2.0 ($\pm$ 1.1) PgCyr^{-1} in time period 2001-2014. The global land sink of JSBACH is approximately -1.7 PgCyr^{-1} (Table 2) and is therefore lower than the land sink by CTE2016. Since the ocean fluxes are a posteriori fluxes from CTE2016 simulation, they cause a bias to the simulated atmospheric CO_2 mole fraction when used together with the land fluxes from the JSBACH simulation. The net land sink of YAS version is slightly closer to CTE2016 value, and this leads to lower bias also at Mauna Loa (Fig. S10).

Additionally, the spaceborn observations also contain bias. GOSAT retrievals were evaluated against ground-based Total Carbon Column Observing Network (TCCON), and XCO_2 is biased low by approximately 1.48 ppm (Yoshida et al., 2013).

In this study we concentrated on analysing the SCAs and the pattern of the seasonal cycle and emphasized the differences between the two different soil carbon models. Therefore we do not consider this bias to play a big role in these analysis.

https://doi.org/10.5194/bg-2020-7
Preprint. Discussion started: 10 February 2020

Also the transport model contains biases (Gurney et al., 2004), but since only one transport model was used in this study, it is expected that the biases are similar between the two model runs and are not the cause for the large differences seen in the two different simulations.

5 Conclusions

We demonstrated how atmospheric CO_2 observations can be used to benchmark soil carbon models and that it is important to benchmark models across several different variables. This work highlighted the importance of the model drivers and their functional dependencies. The YAS model better captured the magnitude and spatial distribution of soil carbon stocks globally and resulted in similar global turnover rate compared to other Earth System Models, in comparison to the much higher turnover rate by the CBA model.

The YAS model showed biases in the atmospheric CO_2 cycle at temperate latitudes in the Northern Hemisphere. The CBA model showed better performance in capturing the seasonal cycle pattern of the CO_2 mole fraction, but it had biases in the high latitudes in the Northern Hemisphere. When considering both land based and atmospheric based observations, it is not straightforward to say which model performed better. However, the R_h from the YAS model showed misalignment with soil water content in the tropical regions, as they were negatively correlated with each other. This suggests that use of precipitation as a proxy for soil moisture might not be sensible in sub-annual time scales.

In addition to the surface observations of CO_2, also space-born XCO_2 observations were used. They were providing a larger-scale confirmation for the results obtained from the surface observations and thus worked as a complimentary information source.

Soil carbon models have several development needs (Bradford et al., 2016; van Groenigen et al., 2017) that are now partly being answered with the next generation models including more mechanistic representation of several below ground processes (Wieder et al., 2015; Yu et al., 2019). The development of moisture dependency from simple empiric relationships is moving towards mechanistic approaches, which may yield more reliable results in the long term (Yan et al., 2018).

Code and data availability. The site level data from Global Atmospheric Watch -network is available via Obspack (2016) (https://doi.org/10.15138/G3059Z). The EDGAR4.2 emission database is available at http://edgar.jrc.ec.europa.eu. The GOSAT data are from GOSAT Data Archive Service (GDAS) (https://data2.gosat.nies.go.jp/index_en.html). The CRUNCEP data is available from Viovy (2010) (https://vesg.ipsl.upmc.fr/thredds/catalog/store/p529viov/cruncep/V7_1901_2015/catalog.html). The JSBACH model can be obtained from the Max Planck Institute for Meteorology, and it is available for the scientific community under the MPI-M Sofware License Agreement (http://www.mpimet.mpg.de/en/science/models/license/, last access: 16 September 2019). The CarbonTracker Europe code is continuously updated and available through a GIT repository at Wageningen University and Research: https://git.wur.nl/ctdas. For further details, see also: www.carbontracker.eu. For the curve fitting for the atmospheric CO_2 data we used scripts available from ERSL NOAA at https://www.esrl.noaa.gov/gmd/ccgg/mbl/crvfit/crvfit.html.

https://doi.org/10.5194/bg-2020-7
Preprint. Discussion started: 10 February 2020

Appendix A: Box model

A simple box model calculation was performed to evaluate the importance of the dependencies on environmental drivers and the soil carbon pool sizes on the larger global seasonal cycle amplitude in R_h as predicted by YAS. In this box model, we assume that heterotophic respiration R_h is a product of environmental dependencies and the turnover time as

$$R_{h,YAS} = b * f_{YAS,T_{air}}(T_{air}) * f_{YAS,P_a}(P_a) * \frac{C_{soil,YAS}}{\tau_{YAS}}, \text{where} \qquad b = \frac{\Sigma f_{CBA,T_{soil}}(T_{soil}) f_{CBA,\alpha}(\alpha)}{\Sigma f_{YAS,T_{air}}(T_{air}) f_{YAS,P_a}(P_a)}, \tag{A1}$$

where $R_{h,YAS}$ is the heterotophic respiration of model YAS, b is a scalar that takes into account the different magnitudes of the response functions, T_{air} is the air temperature, P_a is the annual precipitation, $C_{soil,YAS}$ are the total soil carbon pools and τ_{YAS} is the turnover time of the total soil carbon pools. T_{soil} is the soil temperature and α is the relative soil moisture. This formulation in A1 refers to the YAS model. The response functions are as shown in Section 2.1.2. For the CBA model the formulation is as

$$R_{h,CBA} = \frac{1}{b} * f_{CBA,T_{soil}}(T_{soil}) * f_{CBA,\alpha}(\alpha) * \frac{C_{soil,CBA}}{\tau_{CBA}}. \tag{A2}$$

These response have been introduced in Section 2.1.1.

The equations were used for monthly data averaged over the years 2001-2014 of heterotrophic respiration, environmental drivers and soil carbon stocks to estimate the turnover times for each grid point for YAS using eq. A1 and for CBA using eq. A2. Using these turnover times, we calculated the global R_h with the turnover times and soil carbon pools of each model by making different tests. First, we used the environmental responses and drivers of the other model (lines B in Table A1). Additionally we changed the driving variables, but kept the original response functions (lines C in Table A1). Then we changed only the response functions of the original model while keeping the original driving variables (lines D in Table A1).

Since the driving variables of soil moisture and annual precipitation differed in magnitudes approximately four-fold, the soil moisture was multiplied by four when using the function for annual precipitation (f_{YAS,P_a}) and when annual precipitation was used in the function for soil moisture ($f_{CBA,\alpha}$) it was divided by four. The annual cycles of R_h are shown in Fig. A1 and the amplitudes in Table A1.

Author contributions. TT designed the experiment with the help of SZ. JESM performed the JSBACH model simulations. AT did the CarbonTracker Europe (CTE2016) runs with the JSBACH biospheric fluxes, with the CO_2 fields provided by ITK. ITK provided the CarbonTracker Europe (CTE2016) results used for comparison at the surface stations. TT performed the analysis with help from SZ, AT and TM. TT wrote the first version of the draft and all the authors contributed to the manuscript.

Competing interests. Dr. Sönke Zaehle is an associate editor for Biogeosciences.

https://doi.org/10.5194/bg-2020-7
Preprint. Discussion started: 10 February 2020

Acknowledgements. TT was funded by Academy of Finland (grant no. 266803). TT and SZ were funded by European Research Council (ERC) under the European Union's Horizon 2020 research and innovation programme (QUINCY; grant no. 647204). SZ was furthermore supported by the European Union's Horizon 2020 Project funded under the programme SC5-01-2014 (CRESCENDO, grant No. 641816). ITL received funding from Netherlands Organisation for Scientific Research (NWO) under contract no. 016.Veni.171.095. JEMSN and JP were supported by the German Research Foundation's Emmy Noether Program (PO1751/1-1). JSBACH simulations were conducted at the German Climate Computing Center (DKRZ; allocation bm0891). We thank Dr. Janne Hakkarainen for helping in analysing the GOSAT data and averaging kernel calculation. We thank Dr. Martin Jung for access to the FLUXCOM results and the FLUXCOM initiative. We thank Prof. Dr. Wouter Peters for constructive comments on an earlier version of this manuscript.

https://doi.org/10.5194/bg-2020-7
Preprint. Discussion started: 10 February 2020

References

Bond-Lamberty, B. and Thomson, A.: A global database of soil respiration data, Biogeosciences, 7, 1915–1926, https://doi.org/10.5194/bg-7-1915-2010, http://www.biogeosciences.net/7/1915/2010/, 2010.

Bond-Lamberty, B., Epron, D., Harden, J., Harmon, M. E., Hoffman, F., Kumar, J., David McGuire, A., and Vargas, R.: Estimating heterotrophic respiration at large scales: challenges, approaches, and next steps, Ecosphere, 7, e01 380, https://doi.org/10.1002/ecs2.1380, http://doi.wiley.com/10.1002/ecs2.1380, 2016.

Bradford, M. A., Wieder, W. R., Bonan, G. B., Fierer, N., Raymond, P. A., and Crowther, T. W.: Managing uncertainty in soil carbon feedbacks to climate change, Nature Climate Change, 6, 751–758, https://doi.org/10.1038/nclimate3071, http://www.nature.com/articles/nclimate3071, 2016.

Cadule, P., Friedlingstein, P., Bopp, L., Sitch, S., Jones, C. D., Ciais, P., Piao, S. L., and Peylin, P.: Benchmarking coupled climate-carbon models against long-term atmospheric CO_2 measurements: Coupled climate-carbon models benchmarks, Global Biogeochemical Cycles, 24, n/a–n/a, https://doi.org/10.1029/2009GB003556, http://doi.wiley.com/10.1029/2009GB003556, 2010.

Crowell, S., Baker, D., Schuh, A., Basu, S., Jacobson, A. R., Chevallier, F., Liu, J., Deng, F., Feng, L., McKain, K., Chatterjee, A., Miller, J. B., Stephens, B. B., Eldering, A., Crisp, D., Schimel, D., Nassar, R., O'Dell, C. W., Oda, T., Sweeney, C., Palmer, P. I., and Jones, D. B. A.: The 2015–2016 carbon cycle as seen from OCO-2 and the global in situ network, Atmospheric Chemistry and Physics, 19, 9797–9831, https://doi.org/10.5194/acp-19-9797-2019, https://www.atmos-chem-phys.net/19/9797/2019/, 2019.

Crowther, T. W., Todd-Brown, K. E. O., Rowe, C. W., Wieder, W. R., Carey, J. C., Machmuller, M. B., Snoek, B. L., Fang, S., Zhou, G., Allison, S. D., Blair, J. M., Bridgham, S. D., Burton, A. J., Carrillo, Y., Reich, P. B., Clark, J. S., Classen, A. T., Dijkstra, F. A., Elberling, B., Emmett, B. A., Estiarte, M., Frey, S. D., Guo, J., Harte, J., Jiang, L., Johnson, B. R., Kröel-Dulay, G., Larsen, K. S., Laudon, H., Lavallee, J. M., Luo, Y., Lupascu, M., Ma, L. N., Marhan, S., Michelsen, A., Mohan, J., Niu, S., Pendall, E., Peñuelas, J., Pfeifer-Meister, L., Poll, C., Reinsch, S., Reynolds, L. L., Schmidt, I. K., Sistla, S., Sokol, N. W., Templer, P. H., Treseder, K. K., Welker, J. M., and Bradford, M. A.: Quantifying global soil carbon losses in response to warming, Nature, 540, 104–108, https://doi.org/10.1038/nature20150, http://www.nature.com/articles/nature20150, 2016.

Dalmonech, D. and Zaehle, S.: Towards a more objective evaluation of modelled land-carbon trends using atmospheric CO_2 and satellite-based vegetation activity observations, Biogeosciences, 10, 4189–4210, https://doi.org/10.5194/bg-10-4189-2013, https://www.biogeosciences.net/10/4189/2013/, 2013.

Dee, D. P., Uppala, S. M., Simmons, A. J., Berrisford, P., Poli, P., Kobayashi, S., Andrae, U., Balmaseda, M. A., Balsamo, G., Bauer, P., Bechtold, P., Beljaars, A. C. M., van de Berg, L., Bidlot, J., Bormann, N., Delsol, C., Dragani, R., Fuentes, M., Geer, A. J., Haimberger, L., Healy, S. B., Hersbach, H., Hólm, E. V., Isaksen, L., Kållberg, P., Köhler, M., Matricardi, M., McNally, A. P., Monge-Sanz, B. M., Morcrette, J.-J., Park, B.-K., Peubey, C., de Rosnay, P., Tavolato, C., Thépaut, J.-N., and Vitart, F.: The ERA-Interim reanalysis: configuration and performance of the data assimilation system, Quarterly Journal of the Royal Meteorological Society, 137, 553–597, https://doi.org/10.1002/qj.828, http://doi.wiley.com/10.1002/qj.828, 2011.

EDGAR4.2: Emission Database for Global Atmospheric Research (EDGAR), release version 4.2, European Commission, Joint Research Centre (JRC)/PBL Netherlands Environmental Assessment Agency, 2011.

Exbrayat, J.-F., Pitman, A. J., Zhang, Q., Abramowitz, G., and Wang, Y.-P.: Examining soil carbon uncertainty in a global model: response of microbial decomposition to temperature, moisture and nutrient limitation, Biogeosciences, 10, 7095–7108, https://doi.org/10.5194/bg-10-7095-2013, https://www.biogeosciences.net/10/7095/2013/, 2013.

https://doi.org/10.5194/bg-2020-7
Preprint. Discussion started: 10 February 2020

Giorgetta, M. A., Jungclaus, J., Reick, C. H., Legutke, S., Bader, J., Böttinger, M., Brovkin, V., Crueger, T., Esch, M., Fieg, K., Glushak, K., Gayler, V., Haak, H., Hollweg, H.-D., Ilyina, T., Kinne, S., Kornblueh, L., Matei, D., Mauritsen, T., Mikolajewicz, U., Mueller, W., Notz, D., Pithan, F., Raddatz, T., Rast, S., Redler, R., Roeckner, E., Schmidt, H., Schnur, R., Segschneider, J., Six, K. D., Stockhause, M., Timmreck, C., Wegner, J., Widmann, H., Wieners, K.-H., Claussen, M., Marotzke, J., and Stevens, B.: Climate and carbon cycle changes from 1850 to 2100 in MPI-ESM simulations for the Coupled Model Intercomparison Project phase 5: Climate Changes in MPI-ESM, Journal of Advances in Modeling Earth Systems, 5, 572–597, https://doi.org/10.1002/jame.20038, http://doi.wiley.com/10.1002/jame.20038, 2013.

Giorgetta, M. A., Brokopf, R., Crueger, T., Esch, M., Fiedler, S., Helmert, J., Hohenegger, C., Kornblueh, L., Köhler, M., Manzini, E., Mauritsen, T., Nam, C., Raddatz, T., Rast, S., Reinert, D., Sakradzija, M., Schmidt, H., Schneck, R., Schnur, R., Silvers, L., Wan, H., Zängl, G., and Stevens, B.: ICON-A, the Atmosphere Component of the ICON Earth System Model: I. Model Description, Journal of Advances in Modeling Earth Systems, 10, 1613–1637, https://doi.org/10.1029/2017MS001242, https://agupubs.onlinelibrary.wiley.com/doi/abs/10.1029/2017MS001242, 2018.

Goll, D. S., Brovkin, V., Parida, B. R., Reick, C. H., Kattge, J., Reich, P. B., van Bodegom, P. M., and Niinemets, U.: Nutrient limitation reduces land carbon uptake in simulations with a model of combined carbon, nitrogen and phosphorus cycling, Biogeosciences, 9, 3547–3569, https://doi.org/10.5194/bg-9-3547-2012, https://www.biogeosciences.net/9/3547/2012/, 2012.

Goll, D. S., Brovkin, V., Liski, J., Raddatz, T., Thum, T., and Todd-Brown, K. E. O.: Strong dependence of CO_2 emissions from anthropogenic land cover change on initial land cover and soil carbon parametrization, Global Biogeochemical Cycles, 29, 1511–1523, https://doi.org/10.1002/2014GB004988, https://onlinelibrary.wiley.com/doi/abs/10.1002/2014GB004988, 2015.

Gurney, K. R., Law, R. M., Denning, A. S., Rayner, P. J., Pak, B. C., Baker, D., Bousquet, P., Bruhwiler, L., Chen, Y.-H., Ciais, P., Fung, I. Y., Heimann, M., John, J., Maki, T., Maksyutov, S., Peylin, P., Prather, M., and Taguchi, S.: Transcom 3 inversion intercomparison: Model mean results for the estimation of seasonal carbon sources and sinks: T3 seasonal results, Global Biogeochemical Cycles, 18, n/a–n/a, https://doi.org/10.1029/2003GB002111, http://doi.wiley.com/10.1029/2003GB002111, 2004.

Hashimoto, S., Carvalhais, N., Ito, A., Migliavacca, M., Nishina, K., and Reichstein, M.: Global spatiotemporal distribution of soil respiration modeled using a global database, Biogeosciences, 12, 4121–4132, https://doi.org/10.5194/bg-12-4121-2015, https://www.biogeosciences.net/12/4121/2015/, 2015.

Hernández, L., Jandl, R., Blujdea, V. N. B., Lehtonen, A., Kriiska, K., Alberdi, I., Adermann, V., Cañellas, I., and Didion, M.: Towards complete and harmonized assessment of soil carbon stocks and balance in forests: The ability of the Yasso07 model across a wide gradient of climatic and forest conditions in Europe, Science of Total Environment, p. 12, 2017.

Huijnen, V., Williams, J., van Weele, M., van Noije, T., Krol, M., Dentener, F., Segers, A., Houweling, S., Peters, W., de Laat, J., Boersma, F., Bergamaschi, P., van Velthoven, P., Le Sager, P., Eskes, H., Alkemade, F., Scheele, R., Nédélec, P., and Pätz, H.-W.: The global chemistry transport model TM5: description and evaluation of the tropospheric chemistry version 3.0, Geoscientific Model Development, 3, 445–473, https://doi.org/10.5194/gmd-3-445-2010, http://www.geosci-model-dev.net/3/445/2010/, 2010.

Hursh, A., Ballantyne, A., Cooper, L., Maneta, M., Kimball, J., and Watts, J.: The sensitivity of soil respiration to soil temperature, moisture, and carbon supply at the global scale, Global Change Biology, 23, 2090–2103, https://doi.org/10.1111/gcb.13489, http://doi.wiley.com/10.1111/gcb.13489, 2017.

Hurtt, G. C., Chini, L. P., Frolking, S., Betts, R. A., Feddema, J., Fischer, G., Fisk, J. P., Hibbard, K., Houghton, R. A., Janetos, A., Jones, C. D., Kindermann, G., Kinoshita, T., Klein Goldewijk, K., Riahi, K., Shevliakova, E., Smith, S., Stehfest, E., Thomson, A., Thornton, P., van Vuuren, D. P., and Wang, Y. P.: Harmonization of land-use scenarios for the period 1500–2100: 600 years of global gridded annual

https://doi.org/10.5194/bg-2020-7
Preprint. Discussion started: 10 February 2020

land-use transitions, wood harvest, and resulting secondary lands, Climatic Change, 109, 117, https://doi.org/10.1007/s10584-011-0153-2, https://doi.org/10.1007/s10584-011-0153-2, 2011.

Jung, M., Schwalm, C., Migliavacca, M., Walther, S., Camps-Valls, G., Koirala, S., Anthoni, P., Besnard, S., Bodesheim, P., Carvalhais, N., Chevallier, F., Gans, F., Groll, D. S., Haverd, V., Ichii, K., Jain, A. K., Liu, J., Lombardozzi, D., Nabel, J. E. M. S., Nelson, J. A., Pallandt, M., Papale, D., Peters, W., Pongratz, J., Rödenbeck, C., Sitch, S., Tramontana, G., Weber, U., Reichstein, M., Koehler, P., O'Sullivan, M., and Walker, A.: Scaling carbon fluxes from eddy covariance sites to globe: Synthesis and evaluation of the FLUXCOM approach, Biogeosciences Discussions, 2019, 1–40, https://doi.org/10.5194/bg-2019-368, https://www.biogeosciences-discuss.net/bg-2019-368/, 2019.

Knorr, W.: Annual and interannual CO2 exchanges of the terrestrial biosphere: process-based simulations and uncertainties, Global Ecology and Biogeography, 9, 225–252, https://doi.org/10.1046/j.1365-2699.2000.00159.x, http://doi.wiley.com/10.1046/j.1365-2699.2000.00159.x, 2000.

Koffi, E. N., Rayner, P. J., Scholze, M., and Beer, C.: Atmospheric constraints on gross primary productivity and net ecosystem productivity: Results from a carbon-cycle data assimilation system, Global Biogeochemical Cycles, 26, https://doi.org/10.1029/2010GB003900, https://agupubs.onlinelibrary.wiley.com/doi/abs/10.1029/2010GB003900, 2012.

Krol, M., Houweling, S., Bregman, B., and Bergamaschi, P.: The two-way nested global chemistry-transport zoom model TM5: algorithm and applications, Atmos. Chem. Phys., p. 16, 2005.

Kuze, A., Suto, H., Nakajima, M., and Hamazaki, T.: Thermal and near infrared sensor for carbon observation Fourier-transform spectrometer on the Greenhouse Gases Observing Satellite for greenhouse gases monitoring, Applied Optics, 48, 6716, https://doi.org/10.1364/AO.48.006716, https://www.osapublishing.org/abstract.cfm?URI=ao-48-35-6716, 2009.

Le Quéré, C., Moriarty, R., Andrew, R. M., Canadell, J. G., Sitch, S., Korsbakken, J. I., Friedlingstein, P., Peters, G. P., Andres, R. J., Boden, T. A., Houghton, R. A., House, J. I., Keeling, R. F., Tans, P., Arneth, A., Bakker, D. C. E., Barbero, L., Bopp, L., Chang, J., Chevallier, F., Chini, L. P., Ciais, P., Fader, M., Feely, R. A., Gkritzalis, T., Harris, I., Hauck, J., Ilyina, T., Jain, A. K., Kato, E., Kitidis, V., Klein Goldewijk, K., Koven, C., Landschützer, P., Lauvset, S. K., Lefèvre, N., Lenton, A., Lima, I. D., Metzl, N., Millero, F., Munro, D. R., Murata, A., Nabel, J. E. M. S., Nakaoka, S., Nojiri, Y., O'Brien, K., Olsen, A., Ono, T., Pérez, F. F., Pfeil, B., Pierrot, D., Poulter, B., Rehder, G., Rödenbeck, C., Saito, S., Schuster, U., Schwinger, J., Séférian, R., Steinhoff, T., Stocker, B. D., Sutton, A. J., Takahashi, T., Tilbrook, B., van der Laan-Luijkx, I. T., van der Werf, G. R., van Heuven, S., Vandemark, D., Viovy, N., Wiltshire, A., Zaehle, S., and Zeng, N.: Global Carbon Budget 2015, Earth System Science Data, 7, 349–396, https://doi.org/10.5194/essd-7-349-2015, https://www.earth-syst-sci-data.net/7/349/2015/, 2015.

Le Quéré, C., Andrew, R. M., Friedlingstein, P., Sitch, S., Hauck, J., Pongratz, J., Pickers, P. A., Korsbakken, J. I., Peters, G. P., Canadell, J. G., Arneth, A., Arora, V. K., Barbero, L., Bastos, A., Bopp, L., Chevallier, F., Chini, L. P., Ciais, P., Doney, S. C., Gkritzalis, T., Goll, D. S., Harris, I., Haverd, V., Hoffman, F. M., Hoppema, M., Houghton, R. A., Hurtt, G., Ilyina, T., Jain, A. K., Johannessen, T., Jones, C. D., Kato, E., Keeling, R. F., Goldewijk, K. K., Landschützer, P., Lefèvre, N., Lienert, S., Liu, Z., Lombardozzi, D., Metzl, N., Munro, D. R., Nabel, J. E. M. S., Nakaoka, S.-i., Neill, C., Olsen, A., Ono, T., Patra, P., Peregon, A., Peters, W., Peylin, P., Pfeil, B., Pierrot, D., Poulter, B., Rehder, G., Resplandy, L., Robertson, E., Rocher, M., Rödenbeck, C., Schuster, U., Schwinger, J., Séférian, R., Skjelvan, I., Steinhoff, T., Sutton, A., Tans, P. P., Tian, H., Tilbrook, B., Tubiello, F. N., van der Laan-Luijkx, I. T., van der Werf, G. R., Viovy, N., Walker, A. P., Wiltshire, A. J., Wright, R., Zaehle, S., and Zheng, B.: Global Carbon Budget 2018, Earth System Science Data, 10, 2141–2194, https://doi.org/10.5194/essd-10-2141-2018, https://www.earth-syst-sci-data.net/10/2141/2018/, 2018.

https://doi.org/10.5194/bg-2020-7
Preprint. Discussion started: 10 February 2020

MacBean, N., Maignan, F., Bacour, C., Lewis, P., Peylin, P., Guanter, L., Köhler, P., Gómez-Dans, J., and Disney, M.: Strong constraint on modelled global carbon uptake using solar-induced chlorophyll fluorescence data, Scientific Reports, 8, 1973, https://doi.org/10.1038/s41598-018-20024-w, http://www.nature.com/articles/s41598-018-20024-w, 2018.

Maksyutov, S., Takagi, H., Valsala, V. K., Saito, M., Oda, T., Saeki, T., Belikov, D. A., Saito, R., Ito, A., Yoshida, Y., Morino, I., Uchino, O., Andres, R. J., and Yokota, T.: Regional CO_2flux estimates for 2009–2010 based on GOSAT and ground-based CO_2 observations, Atmospheric Chemistry and Physics, 13, 9351–9373, https://doi.org/10.5194/acp-13-9351-2013, https://www.atmos-chem-phys.net/13/9351/2013/, 2013.

Mauritsen, T., Bader, J., Becker, T., Behrens, J., Bittner, M., Brokopf, R., Brovkin, V., Claussen, M., Crueger, T., Esch, M., Fast, I., Fiedler, S., Fläschner, D., Gayler, V., Giorgetta, M., Goll, D. S., Haak, H., Hagemann, S., Hedemann, C., Hohenegger, C., Ilyina, T., Jahns, T., Jimenéz-de-la-Cuesta, D., Jungclaus, J., Kleinen, T., Kloster, S., Kracher, D., Kinne, S., Kleberg, D., Lasslop, G., Kornblueh, L., Marotzke, J., Matei, D., Meraner, K., Mikolajewicz, U., Modali, K., Möbis, B., Müller, W. A., Nabel, J. E. M. S., Nam, C. C. W., Notz, D., Nyawira, S., Paulsen, H., Peters, K., Pincus, R., Pohlmann, H., Pongratz, J., Popp, M., Raddatz, T. J., Rast, S., Redler, R., Reick, C. H., Rohrschneider, T., Schemann, V., Schmidt, H., Schnur, R., Schulzweida, U., Six, K. D., Stein, L., Stemmler, I., Stevens, B., Storch, J., Tian, F., Voigt, A., Vrese, P., Wieners, K., Wilkenskjeld, S., Winkler, A., and Roeckner, E.: Developments in the MPI-M Earth System Model version 1.2 (MPI-ESM1.2) and Its Response to Increasing CO_2, Journal of Advances in Modeling Earth Systems, 11, 998–1038, https://doi.org/10.1029/2018MS001400, https://onlinelibrary.wiley.com/doi/abs/10.1029/2018MS001400, 2019.

Nabel, J. E. M. S., Naudts, K., and Pongratz, J.: Accounting for forest age in the tile-based dynamic global vegetation model JSBACH4 (4.20p7; git feature/forests) – a land surface model for the ICON-ESM, Geoscientific Model Development Discussions, 2019, 1–24, https://doi.org/10.5194/gmd-2019-68, https://www.geosci-model-dev-discuss.net/gmd-2019-68/, 2019.

ObsPack: Global Atmospheric Data Integration Project, Multi-laboratory compilation of atmospheric carbon dioxide data for the period 1957–2015, $obspack\_co2\_1\_GLOBALVIEWplus\_v2.1\_2016-09-02$, NOAA Earth System Research Laboratory, Global Monitoring Division, 2016.

Peng, S., Ciais, P., Chevallier, F., Peylin, P., Cadule, P., Sitch, S., Piao, S., Ahlström, A., Huntingford, C., Levy, P., Li, X., Liu, Y., Lomas, M., Poulter, B., Viovy, N., Wang, T., Wang, X., Zaehle, S., Zeng, N., Zhao, F., and Zhao, H.: Benchmarking the seasonal cycle of CO_2 fluxes simulated by terrestrial ecosystem models: Seasonal cycle of CO_2 fluxes, Global Biogeochemical Cycles, 29, 46–64, https://doi.org/10.1002/2014GB004931, http://doi.wiley.com/10.1002/2014GB004931, 2015.

Raddatz, T. J., Reick, C. H., Knorr, W., Kattge, J., Roeckner, E., Schnur, R., Schnitzler, K.-G., Wetzel, P., and Jungclaus, J.: Will the tropical land biosphere dominate the climate–carbon cycle feedback during the twenty-first century?, Climate Dynamics, 29, 565–574, https://doi.org/10.1007/s00382-007-0247-8, http://link.springer.com/10.1007/s00382-007-0247-8, 2007.

Reick, C. H., Raddatz, T., Brovkin, V., and Gayler, V.: Representation of natural and anthropogenic land cover change in MPI-ESM: Land Cover in MPI-ESM, Journal of Advances in Modeling Earth Systems, 5, 459–482, https://doi.org/10.1002/jame.20022, http://doi.wiley.com/10.1002/jame.20022, 2013.

Rödenbeck, C., Houweling, S., Gloor, M., and Heimann, M.: CO_2 flux history 1982–2001 inferred from atmospheric data using a global inversion of atmospheric transport, Atmospheric Chemistry and Physics, 3, 1919–1964, https://doi.org/10.5194/acp-3-1919-2003, https://www.atmos-chem-phys.net/3/1919/2003/, 2003.

Rodgers, C. D. and Connor, B. J.: Intercomparison of remote sounding instruments, Journal of Geophysical Research: Atmospheres, 108, n/a–n/a, https://doi.org/10.1029/2002JD002299, http://doi.wiley.com/10.1029/2002JD002299, 2003.

https://doi.org/10.5194/bg-2020-7
Preprint. Discussion started: 10 February 2020

Scharlemann, J. P., Tanner, E. V., Hiederer, R., and Kapos, V.: Global soil carbon: understanding and managing the largest terrestrial carbon pool, Carbon Management, 5, 81–91, https://doi.org/10.4155/cmt.13.77, http://www.tandfonline.com/doi/abs/10.4155/cmt.13.77, 2014.

Shao, P., Zeng, X., Moore, D. J. P., and Zeng, X.: Soil microbial respiration from observations and Earth System Models, Environmental Research Letters, 8, 034 034, https://doi.org/10.1088/1748-9326/8/3/034034, http://stacks.iop.org/1748-9326/8/i=3/a=034034?key=crossref.8de91620f8b1689fd302f83adce962a1, 2013.

Sitch, S., Friedlingstein, P., Gruber, N., Jones, S. D., Murray-Tortarolo, G., Ahlström, A., Doney, S. C., Graven, H., Heinze, C., Huntingford, C., Levis, S., Levy, P. E., Lomas, M., Poulter, B., Viovy, N., Zaehle, S., Zeng, N., Arneth, A., Bonan, G., Bopp, L., Canadell, J. G., Chevallier, F., Ciais, P., Ellis, R., Gloor, M., Peylin, P., Piao, S. L., Le Quéré, C., Smith, B., Zhu, Z., and Myneni, R.: Recent trends and drivers of regional sources and sinks of carbon dioxide, Biogeosciences, 12, 653–679, https://doi.org/10.5194/bg-12-653-2015, https://www.biogeosciences.net/12/653/2015/, 2015.

Tang, X., Fan, S., Du, M., Zhang, W., Gao, S., Liu, S., Chen, G., Yu, Z., Yao, Y., and Yang, W.: Spatial-and temporal-patterns of global soil heterotrophic respiration in terrestrial ecosystems, Earth System Science Data Discussions, 2019, 1–28, https://doi.org/10.5194/essd-2019-123, https://www.earth-syst-sci-data-discuss.net/essd-2019-123/, 2019.

Thoning, K. W., Tans, P. P., and Komhyr, W. D.: Atmospheric carbon dioxide at Mauna Loa Observatory: 2. Analysis of the NOAA GMCC data, 1974–1985, Journal of Geophysical Research: Atmospheres, 94, 8549–8565, https://doi.org/10.1029/JD094iD06p08549, https://agupubs.onlinelibrary.wiley.com/doi/abs/10.1029/JD094iD06p08549, 1989.

Thum, T., Räisänen, P., Sevanto, S., Tuomi, M., Reick, C., Vesala, T., Raddatz, T., Aalto, T., Järvinen, H., Altimir, N., Pilegaard, K., Nagy, Z., Rambal, S., and Liski, J.: Soil carbon model alternatives for ECHAM5/JSBACH climate model: Evaluation and impacts on global carbon cycle estimates, Journal of Geophysical Research, 116, G02 028, https://doi.org/10.1029/2010JG001612, http://doi.wiley.com/10.1029/2010JG001612, 2011.

Todd-Brown, K. E. O., Randerson, J. T., Post, W. M., Hoffman, F. M., Tarnocai, C., Schuur, E. A. G., and Allison, S. D.: Causes of variation in soil carbon simulations from CMIP5 Earth system models and comparison with observations, Biogeosciences, 10, 1717–1736, https://doi.org/10.5194/bg-10-1717-2013, https://www.biogeosciences.net/10/1717/2013/, 2013.

Todd-Brown, K. E. O., Randerson, J. T., Hopkins, F., Arora, V., Hajima, T., Jones, C., Shevliakova, E., Tjiputra, J., Volodin, E., Wu, T., Zhang, Q., and Allison, S. D.: Changes in soil organic carbon storage predicted by Earth system models during the 21st century, Biogeosciences, 11, 2341–2356, https://doi.org/10.5194/bg-11-2341-2014, https://www.biogeosciences.net/11/2341/2014/, 2014.

Tramontana, G., Jung, M., Schwalm, C. R., Ichii, K., Camps-Valls, G., Ráduly, B., Reichstein, M., Arain, M. A., Cescatti, A., Kiely, G., Merbold, L., Serrano-Ortiz, P., Sickert, S., Wolf, S., and Papale, D.: Predicting carbon dioxide and energy fluxes across global FLUXNET sites with regression algorithms, Biogeosciences, p. 23, 2016.

Tuomi, M., Thum, T., Järvinen, H., Fronzek, S., Berg, B., Harmon, M., Trofymow, J., Sevanto, S., and Liski, J.: Leaf litter decomposition—Estimates of global variability based on Yasso07 model, Ecological Modelling, 220, 3362–3371, https://doi.org/10.1016/j.ecolmodel.2009.05.016, https://linkinghub.elsevier.com/retrieve/pii/S030438000900386X, 2009.

Tuomi, M., Laiho, R., Repo, A., and Liski, J.: Wood decomposition model for boreal forests, Ecological Modelling, 222, 709–718, https://doi.org/10.1016/j.ecolmodel.2010.10.025, https://linkinghub.elsevier.com/retrieve/pii/S0304380010005855, 2011.

van der Laan-Luijkx, I. T., van der Velde, I. R., van der Veen, E., Tsuruta, A., Stanislawska, K., Babenhauserheide, A., Zhang, H. F., Liu, Y., He, W., Chen, H., Masarie, K. A., Krol, M. C., and Peters, W.: The CarbonTracker Data Assimilation Shell (CTDAS) v1.0: implementation and global carbon balance 2001–2015, Geoscientific Model Development, 10, 2785–2800, https://doi.org/10.5194/gmd-10-2785-2017, https://www.geosci-model-dev.net/10/2785/2017/, 2017.

https://doi.org/10.5194/bg-2020-7
Preprint. Discussion started: 10 February 2020

van Groenigen, K. J., Osenberg, C. W., Terrer, C., Carrillo, Y., Dijkstra, F. A., Heath, J., Nie, M., Pendall, E., Phillips, R. P., and Hungate, B. A.: Faster turnover of new soil carbon inputs under increased atmospheric CO_2, Global Change Biology, 23, 4420–4429, https://doi.org/10.1111/gcb.13752, http://doi.wiley.com/10.1111/gcb.13752, 2017.

Viovy, N.: CRU-NCEP dataset, http://dods.extra.cea.fr/data/p529viov/cruncep/readme.htm, 2010.

Wang, H., Jiang, F., Wang, J., Ju, W., and Chen, J. M.: Terrestrial ecosystem carbon flux estimated using GOSAT and OCO-2 XCO $_2$ retrievals, Atmospheric Chemistry and Physics, 19, 12 067–12 082, https://doi.org/10.5194/acp-19-12067-2019, https://www.atmos-chem-phys.net/19/12067/2019/, 2019.

Warner, D., Bond-Lamberty, B., Jian, J., Stell, E., and Vargas, R.: Spatial predictions and associated uncertainty of annual soil respiration at the global scale, Global Biogeochemical Cycles, p. 2019GB006264, https://doi.org/10.1029/2019GB006264, https://onlinelibrary.wiley.com/doi/abs/10.1029/2019GB006264, 2019.

Wei, W.: Forest soil respiration and its heterotrophic and autotrophic components: Global patterns and responses to temperature and precipitation, Soil Biology, p. 9, 2010.

Welp, L. R., Keeling, R. F., Meijer, H. A. J., Bollenbacher, A. F., Piper, S. C., Yoshimura, K., Francey, R. J., Allison, C. E., and Wahlen, M.: Interannual variability in the oxygen isotopes of atmospheric CO_2 driven by El Niño, Nature, 477, 579–582, https://doi.org/10.1038/nature10421, http://www.nature.com/articles/nature10421, 2011.

Wieder, W. R., Cleveland, C. C., Smith, W. K., and Todd-Brown, K.: Future productivity and carbon storage limited by terrestrial nutrient availability, Nature Geoscience, 8, 441–444, https://doi.org/10.1038/ngeo2413, http://www.nature.com/articles/ngeo2413, 2015.

Wieder, W. R., Hartman, M. D., Sulman, B. N., Wang, Y.-P., Koven, C. D., and Bonan, G. B.: Carbon cycle confidence and uncertainty: Exploring variation among soil biogeochemical models, Global Change Biology, 24, 1563–1579, https://doi.org/10.1111/gcb.13979, http://doi.wiley.com/10.1111/gcb.13979, 2018.

Yan, Z., Bond-Lamberty, B., Todd-Brown, K. E., Bailey, V. L., Li, S., Liu, C., and Liu, C.: A moisture function of soil heterotrophic respiration that incorporates microscale processes, Nature Communications, 9, 2562, https://doi.org/10.1038/s41467-018-04971-6, http://www.nature.com/articles/s41467-018-04971-6, 2018.

Yoshida, Y., Kikuchi, N., Morino, I., Uchino, O., Oshchepkov, S., Bril, A., Saeki, T., Schutgens, N., Toon, G. C., Wunch, D., Roehl, C. M., Wennberg, P. O., Griffith, D. W. T., Deutscher, N. M., Warneke, T., Notholt, J., Robinson, J., Sherlock, V., Connor, B., Rettinger, M., Sussmann, R., Ahonen, P., Heikkinen, P., Kyrö, E., Mendonca, J., Strong, K., Hase, F., Dohe, S., and Yokota, T.: Improvement of the retrieval algorithm for GOSAT SWIR XCO_2 and XCH_4 and their validation using TCCON data, Atmospheric Measurement Techniques, 6, 1533–1547, https://doi.org/10.5194/amt-6-1533-2013, https://www.atmos-meas-tech.net/6/1533/2013/, 2013.

Yu, L., Ahrens, B., Wutzler, T., Schrumpf, M., and Zaehle, S.: Jena Soil Model: a microbial soil organic carbon model integrated with nitrogen and phosphorus processes, preprint, Climate and Earth System Modeling, https://doi.org/10.5194/gmd-2019-187, https://www.geosci-model-dev-discuss.net/gmd-2019-187/, 2019.

Ťupek, B., Launiainen, S., Peltoniemi, M., Sievänen, R., Perttunen, J., Kulmala, L., Penttilä, T., Lindroos, A., Hashimoto, S., and Lehtonen, A.: Evaluating CENTURY and Yasso soil carbon models for CO_2 emissions and organic carbon stocks of boreal forest soil with Bayesian multi-model inference, European Journal of Soil Science, p. ejss.12805, https://doi.org/10.1111/ejss.12805, https://onlinelibrary.wiley.com/doi/abs/10.1111/ejss.12805, 2019.

https://doi.org/10.5194/bg-2020-7
Preprint. Discussion started: 10 February 2020

Biogeosciences
Discussions
Open Access
EGU

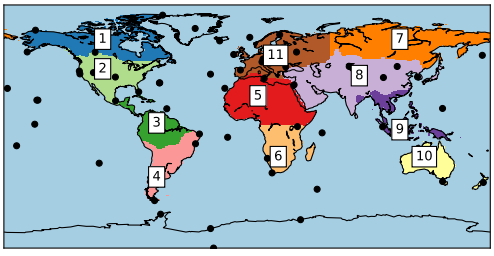

Figure 1. Locations of GAW stations, denoted as black dots, and different TransCom regions as different colors.

https://doi.org/10.5194/bg-2020-7
Preprint. Discussion started: 10 February 2020

Biogeosciences
Discussions
Open Access
EGU

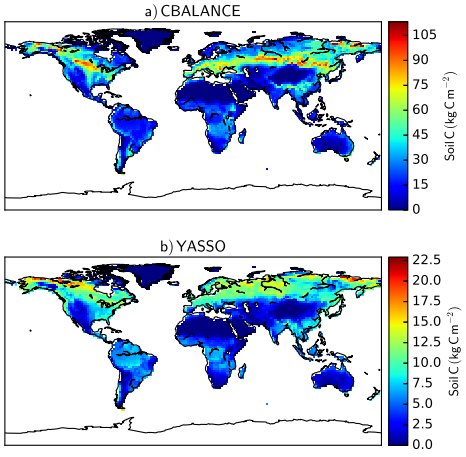

Figure 2. The distribution of total soil carbon globally for CBA (a) and YAS (b). The scales are different between the plots.

https://doi.org/10.5194/bg-2020-7
Preprint. Discussion started: 10 February 2020

Biogeosciences
Discussions
Open Access
EGU

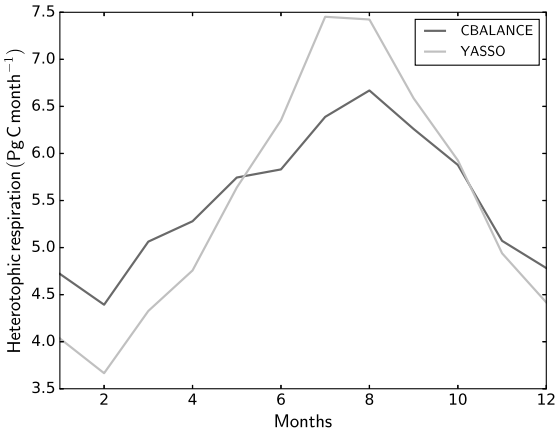

Figure 3. The annual cycle of heterotrophic respiration globally with the CBALANCE (dark grey) and YASSO (light grey) model versions.

https://doi.org/10.5194/bg-2020-7
Preprint. Discussion started: 10 February 2020

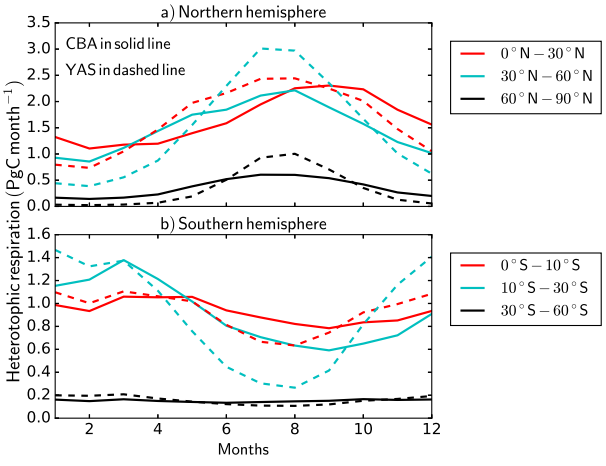

Figure 4. The annual cycle of heterotrophic respiration in Northern (a) and Southern (b) Hemispheres separated into latitudinal zones. CBALANCE results are shown in solid lines and the YASSO results in dashed lines.

https://doi.org/10.5194/bg-2020-7
Preprint. Discussion started: 10 February 2020

Biogeosciences
Discussions
Open Access
EGU

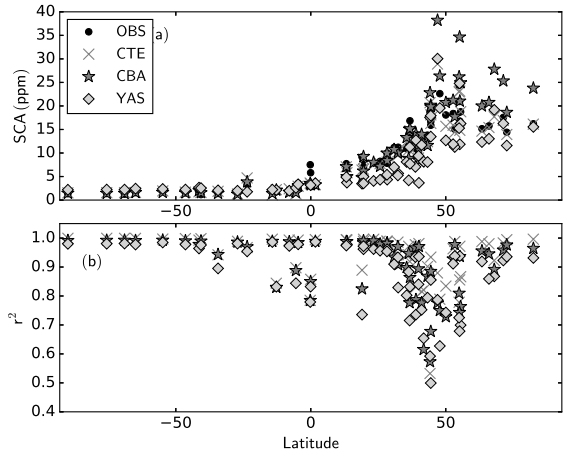

Figure 5. The seasonal cycle amplitudes (SCAs) of atmospheric CO_2 in ppm (a) and r^2 between the simulations and observations (b) at different Global Atmosphere Watch stations as a function of latitude.The black circles denote observations, the grey crosses are the results from the CarbonTracker Europe 2016 (CTE), the dark grey stars are the results from the CBALANCE (CBA) run and the lighter grey diamonds are the results from the YASSO (YAS) run.

https://doi.org/10.5194/bg-2020-7
Preprint. Discussion started: 10 February 2020

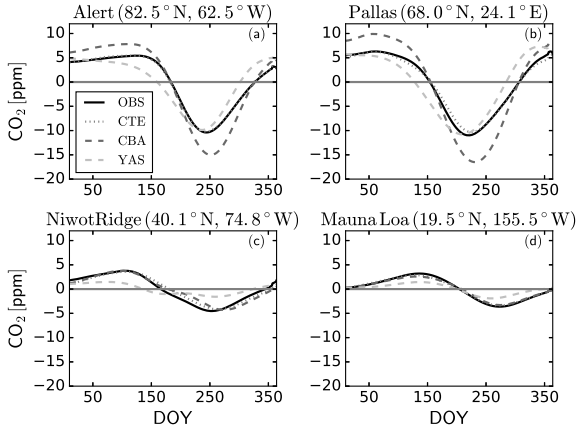

Figure 6. The detrended seasonal cycles of atmospheric CO_2 at four Global Atmospheric Watch sites: Alert (a), Pallas (b), Niwot Ridge (c), Mauna Loa (d) for observations (OBS) in black solid line, CarbonTracker Europe 2016 (CTE) in a grey dotter line, and the two JSBACH model version with CBALANCE (CBA) in dark grey dashed line and YASSO (YAS) in light grey dashed line. The solid grey line denotes the zero line.

https://doi.org/10.5194/bg-2020-7
Preprint. Discussion started: 10 February 2020

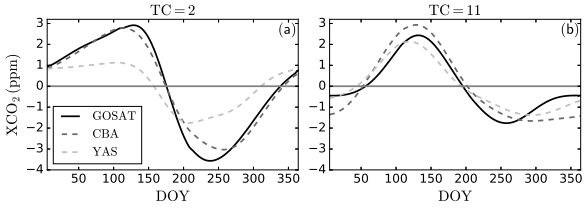

Figure 7. The seasonal cycles of detrended atmospheric XCO_2 mole fraction at TransCom regions two, southern part of North America (a) and eleven, Europe (b). The observations are in black solid line, CBALANCE (CBA) model results in dashed dark grey line and YASSO (YAS) model results in dasher light grey line. The solid grey line denotes the zero line.

https://doi.org/10.5194/bg-2020-7
Preprint. Discussion started: 10 February 2020

Table 1. Global C storage in the two different model formulations averaged over 2001-2014. For the YAS model the eight above ground pools are summed to obtain the litter pool, while the remaining 10 pools (below ground and humus) represent the soil pool.

C pool (Pg C)	CBA	YAS
Litter C	171	263
Soil C	3217	703
Vegetation C	432	432

https://doi.org/10.5194/bg-2020-7
Preprint. Discussion started: 10 February 2020

Table 2. Global terrestrial C fluxes from the two different model formulations averaged over 2001-2014.

Row	Flux ($PgCyear^{-1}$)	CBA	YAS
A	Net CO_2 flux (A = -B + E + G + H + I + J)	-1.68	-1.75
B	GPP	167	same
C	Heterotrophic resp. R_h	66.1	65.5
D	Autotrophic resp. R_a	89.9	same
E	TER (E = C + D)	156	156
F	NPP (F = B - D)	77.4	same
G	Direct land cover change	2.30	same
H	Fire	1.60	2.10
I	Harvest	0.23	same
J	Herbivory	5.54	same

https://doi.org/10.5194/bg-2020-7
Preprint. Discussion started: 10 February 2020

Table 3. r^2 values for the different latitudinal zones between modelled heterotrophic respiration and the environmental drivers of the CBALANCE (CBA) and YASSO (YAS) models. The environmental drivers are all calculated as monthly means for the latitudinal zones. The values denoted by asterisk (*) show a negative correlation. The positive relationships with the r^2 value of 0.80 or more have been written in bold. α is the relative soil moisture, T_{soil} and T_{air} are soil and air temperature, and P_a is the precipitation.

Lat. zone	CBA vs. α	CBA vs. T_{soil}	YAS vs. P_a	YAS vs. T_{air}	YAS vs. α
60°N -90°N	0.04	**0.92**	**0.91**	**0.80**	0.23
30°N -60°N	0.65*	**0.97**	**0.95**	**0.90**	0.85*
0°N -30°N	**0.92**	0.24	**0.92**	**0.86**	0.34
0°S -10°S	**0.84**	0.00	**0.86**	0.27	0.20
10°S -30°S	**0.88**	0.14	**0.87**	**0.82**	0.22
30°S -60°S	0.21*	0.58	0.60	**0.91**	0.83*

https://doi.org/10.5194/bg-2020-7
Preprint. Discussion started: 10 February 2020

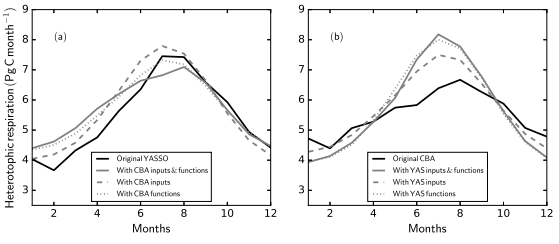

Figure A1. Different annual cycles of the heterotrophic respiration (R_h) predicted by the YASSO (a) and CBALANCE (b) model and the different alternatives from the box model calculation.

https://doi.org/10.5194/bg-2020-7
Preprint. Discussion started: 10 February 2020

Biogeosciences Discussions Open Access EGU

Table A1. The amplitude of global heterotrophic respiration within a year in different box model formulations. The input variables or functions that differ from the original model formulation are in bold letters.

Line	Option	Amplitude ($\mathrm{PgCyear}^{-1}$)
A)	YAS - Original model	3.8
B)	YAS with inputs $\mathbf{T_{soil}}$ and α and functions $\mathbf{f_{CBA,T_{soil}}}$ and $\mathbf{f_{CBA},\alpha}$	2.7
C)	YAS with inputs $\mathbf{T_{soil}}$ and α and functions $f_{YAS,T_{air}}$ and f_{YAS,P_a}	3.7
D)	YAS with inputs T_{air} and P_a and functions $\mathbf{f_{CBA,T_{soil}}}$ and $\mathbf{f_{CBA},\alpha}$	3.0
A)	CBA - Original model	2.3
B)	CBA with inputs $\mathbf{T_{air}}$ and $\mathbf{P_a}$ and functions $\mathbf{f_{YAS,T_{air}}}$ and $\mathbf{f_{YAS,P_a}}$	4.2
C)	CBA with inputs $\mathbf{T_{air}}$ and $\mathbf{P_a}$ and functions $f_{CBA,T_{soil}}$ and f_{CBA},α	3.2
D)	CBA with inputs T_{soil} and α and functions $\mathbf{f_{YAS,T_{air}}}$ and $\mathbf{f_{YAS,P_a}}$	4.0